

Polythiophene Derivative with Phenothiazine–Vinylene Conjugated Side Chain: Synthesis and Its Application in Field-Effect Transistors

Yingping Zou,^{†,‡} Weiping Wu,^{†,‡} Guangyi Sang,^{†,‡} Yi Yang,^{†,‡} Yunqi Liu,^{*,†} and Yongfang Li^{*,†}

Beijing National Laboratory for Molecular Sciences and CAS Key Laboratory of Organic Solids, Institute of Chemistry, Chinese Academy of Sciences (CAS), Beijing 100080, China, and Graduate University of Chinese Academy of Sciences, Beijing 100039, China

Received June 24, 2007; Revised Manuscript Received July 17, 2007

ABSTRACT: A new polythiophene derivative with phenothiazine–vinylene (PTZV) conjugated side chains, **PTZV–PT**, was synthesized through the Stille coupling reaction and characterized by ¹H NMR, elemental analysis, GPC, TGA, DSC, UV–vis absorption spectroscopy, photoluminescence spectroscopy, and cyclic voltammetry. The polymer is soluble in common organic solvents and possesses good thermal stability with 5% weight loss at the temperature of 397 °C and *T*_g of 140 °C. The weight-average molecular weight of **PTZV–PT** was 5.45×10^4 with the polydispersity index of 1.48. The absorption spectrum of **PTZV–PT** film displays a broad plateau between 300 and 600 nm. The hole mobility of **PTZV–PT** determined from space-charge-limited current model was $4.7 \times 10^{-3} \text{ cm}^2 \text{ V}^{-1} \text{ s}^{-1}$. The field effect hole mobility of the polymer reached $6.8 \times 10^{-3} \text{ cm}^2 \text{ V}^{-1} \text{ s}^{-1}$ with an on/off ratio of 2.5×10^4 , which is among the best performance of the regiorandom polymers for the solution-processed organic field effect transistors (OFETs). The preliminary results indicate that **PTZV–PT** is a promising polymer material for applications in solution-processable OFETs.

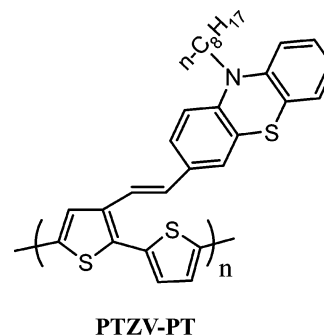
1. Introduction

Conjugated polymers have drawn great attention since the discovery of conducting polyacetylene in 1977. Among the conjugated polymers, polythiophene derivatives (PTs) attracted the most intensive studies for their promising applications in polymer solar cells,^{1–3} light-emitting diodes,^{4–6} and field-effect transistors (FETs).^{7–8} In order to improve the optoelectronic properties to meet the request for different applications, chemical modifications of PTs have been well performed.

Organic field effect transistors (OFETs) attracted broad interest recently because of their promising applications in organic sensors,⁹ integrated circuit, low-cost large area memories, smart cards, and driving circuits for large-area displays.^{10,11} One of the most important aspects for OFETs is that they can be fabricated by easy patterning techniques at low cost and have good compatibility with flexible plastic substrates. Thus, the solution processable polymers are preferable to small molecules. Design and synthesis of new conjugated polymer semiconductors with high charge carrier mobility is highly desirable for the realization of high-performance solution processable OFETs.¹²

For the application of the conjugated polymers in polymer solar cells (PSCs) as the electron donor, broad absorption in the visible region and higher hole mobility of the conjugated polymers are crucial for efficient photovoltaic materials. It is well-known that the increase of effective conjugation length will broaden the absorption of π -conjugated polymers; thus, our group recently synthesized a series of polythiophene and poly-(thienylene vinylene) derivatives with conjugated phenylene–vinylene,¹³ thienylene–vinylene¹⁴ or terthiophene–vinylene¹⁵ side chains. The polymers with the conjugated side chains

Scheme 1. Chemical Structure of the Polythiophene Derivative PTZV–PT



showed broad absorption in the visible region and higher hole mobility.^{13–15}

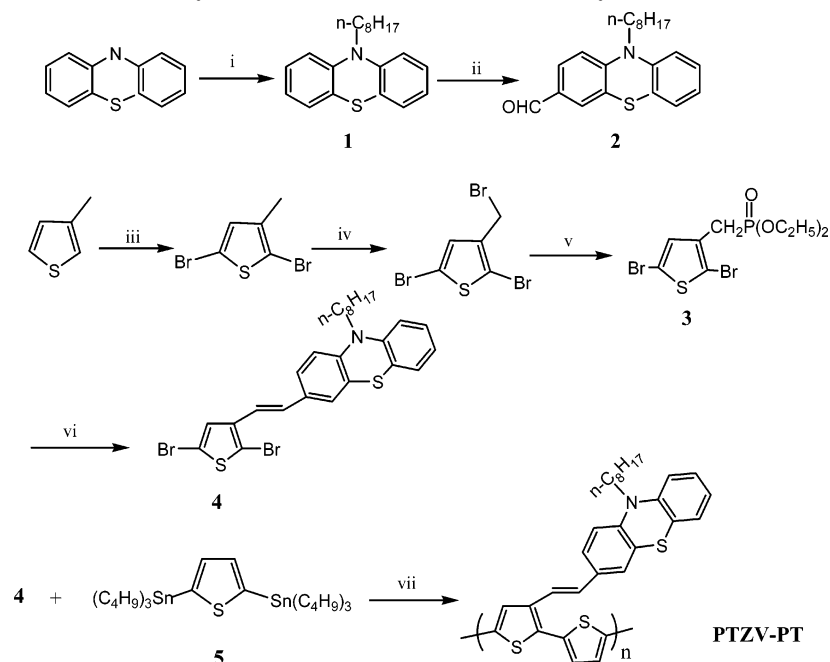
A notable feature of conjugated polymers lies in the versatility of their molecular structure which affords wide space to construct new polymers with improved properties. Phenothiazine is a well-known heterocyclic compound with electron-rich sulfur and nitrogen heteroatoms.^{16,17} Polymers and organic molecules containing phenothiazine or its derivatives possess unique optoelectronic properties for diverse applications such as OFET,¹⁶ light emitting diodes,¹⁸ photovoltaic devices,¹⁹ and chemiluminescence.²⁰ Hwang et al.¹⁶ reported a conjugated copolymer of phenothiazine and fluorene, and the OFET based on the polymer showed a hole field effect mobility of $0.8 \times 10^{-4} \text{ cm}^2 \text{ V}^{-1} \text{ s}^{-1}$ and an on/off ratio of 10^3 .

In order to investigate the effect of side-chain structure on the property of the polythiophene derivatives with conjugated side chains and to develop new conjugated polymers with high hole mobility, we synthesized a new polythiophene derivative with a hole transporting phenothiazine unit^{17b} as conjugated side chains, **PTZV–PT** (see Scheme 1), via the Stille coupling reaction. The hole mobility of **PTZV–PT**, measured by the space-charge-limited current (SCLC) method, reached $4.7 \times$

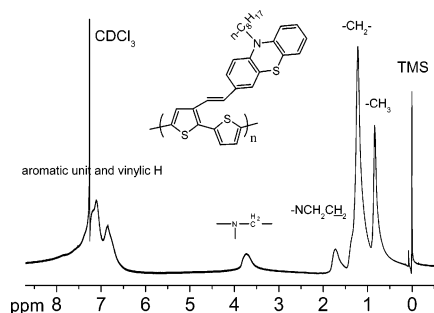
* Corresponding author. E-mail: liyf@iccas.ac.cn (Y.Li.); liuyq@iccas.ac.cn (Y.Liu). Fax: 86-10-62559373.

[†] Beijing National Laboratory for Molecular Sciences and CAS Key Laboratory of Organic Solids, Institute of Chemistry, Chinese Academy of Sciences (CAS).

[‡] Graduate University of Chinese Academy of Sciences.

Scheme 2. Synthetic Route of the Monomers and Polymer PTZV-PT^a

^a Key: (i) $\text{C}_8\text{H}_{17}\text{Br}$, DMSO, NaOH, room temperature, 24 h, 93%; (ii) POCl_3 , DMF, 90 °C, 36 h, 84%; (iii) NBS, $\text{CHCl}_3/\text{HOAc}$, 2 h, 85%; (iv) NBS, BPO, CCl_4 , reflux, 3 h, 83%; (v) $\text{P}(\text{OC}_2\text{H}_5)_3$, 160 °C, 2 h, 70%; (vi) 2, NaOCH_3 , DMF, room temperature, 2 h, 82%; (vii) $\text{Pd}(\text{Ph}_3)_4$, toluene, reflux, 12 h, 72%.

Figure 1. ¹H NMR spectra of the polymer PTZV-PT.

$10^{-3} \text{ cm}^2 \text{ V}^{-1} \text{ s}^{-1}$ which is about three orders higher than that of the common polythiophenes ($10^{-6} \text{ cm}^2 \text{ V}^{-1} \text{ s}^{-1}$). An OFET was fabricated using PTZV-PT as a new p-type channel material and characterized. The hole field effect mobility of the polymer was $6.8 \times 10^{-3} \text{ cm}^2 \text{ V}^{-1} \text{ s}^{-1}$ with an on/off ratio of 2.5×10^4 , which is among the best performances observed for the solution-processed OFETs. Moreover, the absorption spectrum of PTZV-PT film displays a broad plateau from 300 to 600 nm, indicating that the polymer could also be a promising photovoltaic material.

2. Results and Discussion

2.1. Synthesis and Characterization of the Polymer. The synthesis of the monomers and the corresponding polymer are outlined in Scheme 2. Phenothiazine was used as a starting material for the preparation of 1 which was in turn converted to 2 by the Vilsmeier reaction, the monomer 4 was obtained using 2 and 3 in 82% yield by the Wittig-Hornor reaction.²¹

The polymer PTZV-PT was easily prepared by the Stille coupling method¹³ and identified by ¹H NMR spectroscopy (as shown in Figure 1) and elemental analysis. In the ¹H NMR spectra, the characteristic peaks at δ 7.36–6.93 and 6.85–6.52 ppm can be assigned to the resonance of protons on the phenothiazine ring, the thiophene ring, and the vinylene group. The peak due to protons in $-\text{CH}_2-$ linked to nitrogen is at

3.71 ppm; the peaks at δ 1.74–0.84 ppm correspond to the protons of the long alkyl chain. These results, combined with the elemental analysis, indicate that the Stille reaction is successful and complete. The synthesized polymer PTZV-PT was soluble in common organic solvents, such as chloroform, toluene, and xylene at room temperature. The weight-average molecular weight (M_w) of PTZV-PT was 5.4×10^4 with a polydispersity index of 1.48.

Thermal properties of PTZV-PT were investigated by means of DSC and thermogravimetric analysis (TGA) under nitrogen atmosphere, as shown in Figure 2. TGA plot (Figure 2a) reveals that the polymer possesses good thermal stability with the onset decomposition temperature around 300 °C in nitrogen, 5% weight loss at the temperature of 397 °C. Glass transition temperature (T_g) of PTZV-PT is 140 °C, obtained from the DSC analysis (see Figure 2b). Obviously, the thermal stability of the polymer is adequate for the fabrication processes of optoelectronic devices.

2.2. UV-Vis Absorption and PL Spectra. The UV-vis absorption spectra could provide a good deal of information on the electronic structure of the conjugated polymers. Figure 3 shows the absorption spectra of PTZV-PT in dilute chloroform solution and film. For PTZV-PT dilute solution, there are a broad UV absorption peak at around 300 nm and a visible absorption peak at ca. 401 nm with a broad shoulder peak at around 529 nm. In comparison with the absorption spectrum of monomer 4 with three peaks at 280, 308, and 380 nm (also shown in Figure 3), the UV absorption and the peak at 401 nm should be mainly contributed from the phenothiazine vinyl conjugated side chains, the shoulder peak at around 529 nm should be contributed from the polythiophene main chains of the polymer. Probably, the steric hindrance of the big PTZV side chains makes the polymer main chains distorted in solution, so that the main chain absorption is weaker and appears as a shoulder peak. The absorption of the conjugated PTZV side chain of the polymer at 401 nm is red-shifted in comparison with that (ca. 350–370 nm) of phenylene vinyl side chains in

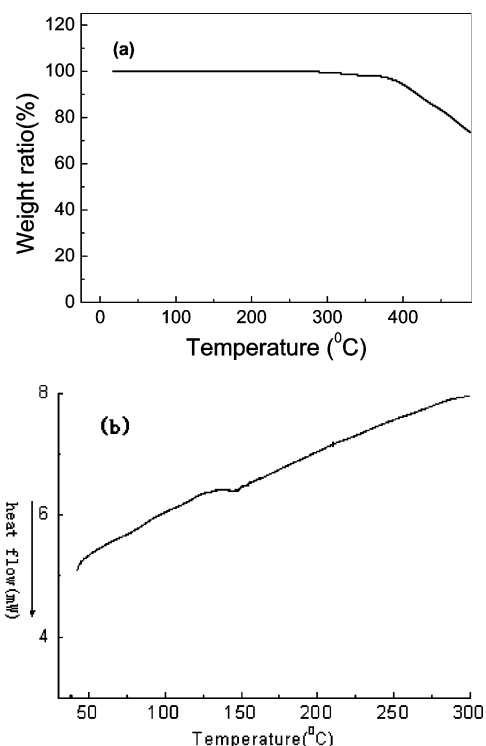


Figure 2. (a) TGA plot and (b) DSC thermogram of **PTZV-PT**.

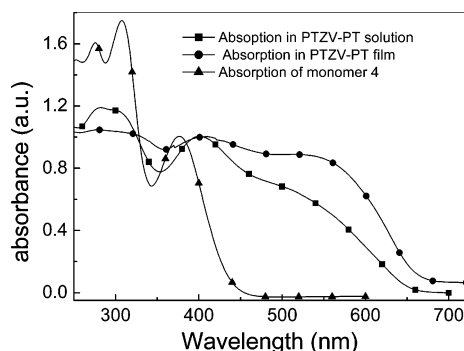


Figure 3. Absorption spectra of the polymer **PTZV-PT** and monomer **4** in dilute solutions in CHCl_3 and **PTZV-PT** film.

the side chain conjugated PTs,^{13a} indicating that the PTZV donor group possesses a higher effective conjugation than that of phenylene vinyl group in the side chain conjugated PTs.

For the absorption spectrum of **PTZV-PT** film, the main chain absorption strengthened and red-shifted to around 550 nm in comparison with the shoulder peak (at 529 nm) of the polymer solution, which results from the strong interchain interactions in the polymer film. In addition, the absorption of **PTZV-PT** film is red-shifted by 70 nm in comparison with that of poly-(3-arylthiophene) where phenylene side chain was connected with PT main chain by saturated linkage,²² indicating that the phenothiazine groups on the side chains extended the absorption window of the polymer through the linkage of the vinyl bond. The **PTZV-PT** film shows a very broad absorption plateau covering the wavelength range from 250 to 650 nm, which is a mixture of three absorption peaks including the UV peak at around 300 nm and the two visible peaks at ca. 410 nm and at around 550 nm. The broad absorption spectra indicate that the polymer could be a promising photovoltaic material.

Figure 4 shows PL spectra of the **PTZV-PT** solution and film. For the polymer solution, the same PL peak at 599 nm was observed when excited at the two wavelengths of 402 nm (corresponding to the absorption of the conjugated side chains)

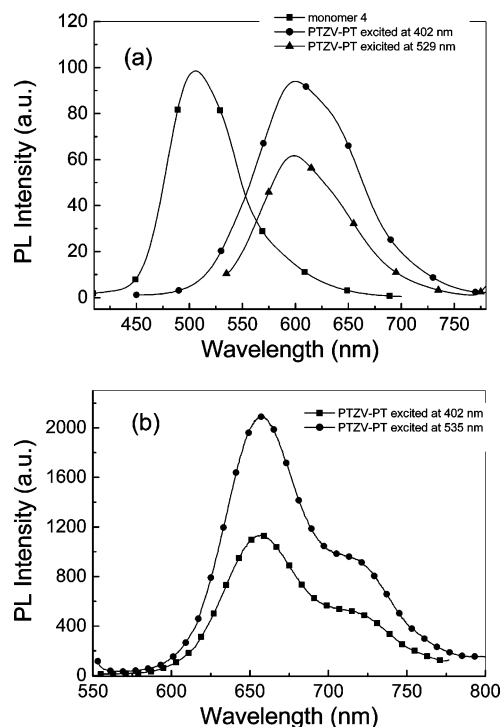


Figure 4. PL spectra of (a) **PTZV-PT** and monomer **4** dilute solutions in CHCl_3 and (b) **PTZV-PT** film.

and 529 nm (corresponding to the absorption of the polymer main chain) respectively. In comparison, monomer **4** exhibits a PL maximum at ca. 500 nm under the excitation at 400 nm. Obviously, the PL peak at 599 nm should come from the emission of the polythiophene main chain of the polymer, while the emission of the PTZV substituted thiophene units at ca. 500 nm (excited at 400 nm) was not observed. The results indicate that the intramolecular exciton energy transfer from the conjugated side chains to the polymer main chains occurred when the conjugated side chains were excited at the wavelength of ca. 400 nm. In the film state, **PTZV-PT** exhibits a PL peak at 660 nm under the excitation of 402 and 535 nm, respectively, which indicates that the intramolecular exciton energy transfer process from the conjugated side chains to the main chains also takes place in the film state, and the PL emission of the polymer film red-shifted by ca. 60 nm than that of the polymer solution due to interchain interaction in the solid film. This phenomenon was also observed from other polythiophene derivatives with conjugated side chains^{13–15} and from the PPV derivative with OXD side chains.²³ The intramolecular exciton energy transfer ensures that all photons absorbed by the polymers are useful for the photovoltaic conversion when the polymer is used as the photovoltaic material.

The relative intensity of the two PL peaks excited at the absorption peak wavelength of conjugated side chain (ca. 400 nm) and polymer main chain (ca. 530 nm) is different for the polymer solution and film. The PL peak excited at 402 nm is stronger than that excited at 529 nm for the polymer dilute solution (see Figure 4a), while the PL peak excited at 402 nm is weaker than that excited at 535 nm for the polymer film (see Figure 4b). The phenomenon could be related to the relatively stronger absorption of the polymer main chain in film state and/or the higher efficiency of the intramolecular exciton energy transfer for the polymer solution than that of the polymer film.

2.3. Electrochemical Properties. Cyclic voltammetry was widely employed to estimate the HOMO and LUMO energy levels of the conjugated polymers, because the onset oxidation

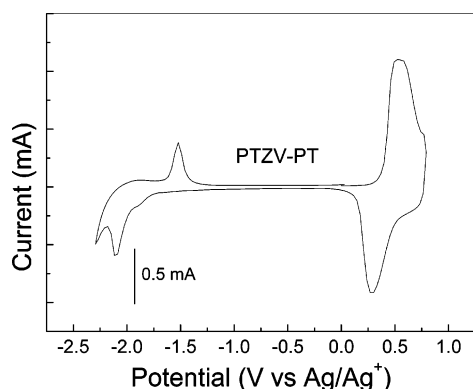


Figure 5. Cyclic voltammogram of **PTZV-PT** film on platinum electrode in a 0.1 mol/L Bu_4NPF_6 CH_3CN solution.

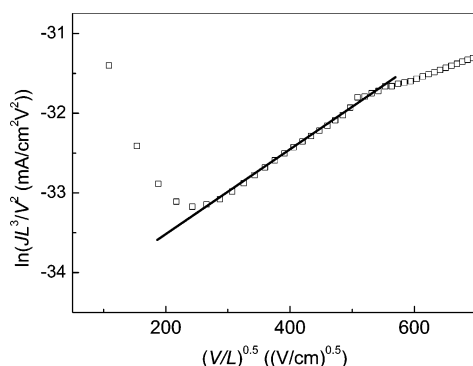


Figure 6. Current–voltage data from the device ITO/PEDOT:PSS/**PTZV-PT**/Au, plotted in the format $\ln(JL^3/V^2)$ vs $(V/L)^{0.5}$, where J is the current density and L is the thickness of the polymer layer. The lines are the fit to the respective experimental points.

and reduction potentials obtained from the cyclic voltammograms correspond to the HOMO and LUMO energy levels, respectively.²⁴ Figure 5 shows the cyclic voltammogram of the **PTZV-PT** film on Pt electrode in 0.1 mol/L Bu_4NPF_6 CH_3CN solution. It can be seen that there are reversible p-doping/dedoping (oxidation/reduction) processes at positive potential range and n-doping/dedoping (reduction/reoxidation) processes at negative potential range. Interestingly, the oxidation (p-doping) current of **PTZV-PT** is obviously higher than that of the reduction (n-doping) current in the cyclic voltammogram, suggesting that **PTZV-PT** with the PTZV conjugated side chain possesses a stronger p-doping ability, that is to say, **PTZV-PT** is an efficient electron-donating material. We can get the HOMO and LUMO levels of **PTZV-PT** from the onset oxidation potential ($E_{\text{on}}^{\text{ox}}$) and onset reduction potential ($E_{\text{on}}^{\text{red}}$) according to the following equations:²⁵ $\text{HOMO} = -e(E_{\text{on}}^{\text{ox}} + 4.71)$ (eV); $\text{LUMO} = -e(E_{\text{on}}^{\text{red}} + 4.71)$ (eV). LUMO and HOMO levels of the polymer calculated from the electrochemical measurement were -4.99 and -2.99 eV respectively. The energy gap of **PTZV-PT** film is 2.0 eV from the difference between the onset oxidation and reduction potentials, which is a little higher than that of the optical energy gap E_g^{opt} (1.81 eV).

2.4. Hole Mobility. Hole mobility of **PTZV-PT** was measured by the space-charge-limited current (SCLC) method²⁶ with a device structure of ITO/PEDOT:PSS/polymer/Au. The results were plotted as $\ln(JL^3/V^2)$ vs $(V/L)^{0.5}$ and shown in Figure 6. The hole mobility of **PTZV-PT** calculated from the data in Figure 6 was $4.7 \times 10^{-3} \text{ cm}^2 \text{ V}^{-1} \text{ s}^{-1}$, which is a relatively higher value among those of the conjugated polymers measured by SCLC method.^{26a,d} This result indicates that the hole transporting phenothiazine unit strongly enhanced the hole mobility of the polymers.

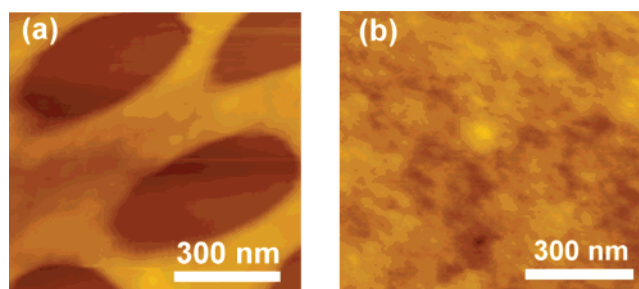


Figure 7. AFM tapping mode topographical images of **PTZV-PT** films on (a) SiO_2 surface and (b) OTS-modified SiO_2/Si substrates.

2.5. Organic Field Effect Transistors. The structure order and crystallization of **PTZV-PT** film was investigated by atomic force microscopy (AFM) and X-ray diffraction (XRD). Figure 7 shows the AFM photographs of **PTZV-PT** films on SiO_2 substrate without and with octadecyltrichlorosilane (OTS) treatment, respectively. Pin holes are commonly observed on the SiO_2 substrate without OTS treatment (Figure 7a), which may be attributed to the sudden evaporation of solvents through a thick polymer layer. **PTZV-PT** film on OTS-modified SiO_2/Si substrates exhibited smoother and more homogeneous morphology (Figure 7b).

To evaluate the crystallinity of the polymer, XRD measurements were taken for the thick spin-coated films on SiO_2 substrate without and with OTS modifications. As shown in Figure 8, both of the two films showed a broad and weak diffraction peak at ca. 21° and there is no peak at the small angle region, revealing that the polymer films were in amorphous form.

The OFETs based on **PTZV-PT** were found to exhibit typical p-type FET characteristics. When bare SiO_2 was used as substrate the field mobility was very low (around $4 \times 10^{-4} \text{ cm}^2 \text{ V}^{-1} \text{ s}^{-1}$) due to the poor film morphology (Figure 7a). OTS modified substrate produced much better morphology (Figure 7b) and improved device performances. The typical current–voltage characteristics of OFETs on the OTS modified SiO_2 substrates are shown in Figure 9. The devices showed ideal transistor performance with apparent saturation behavior, as shown in Figure 9, parts a and b. In the OFETs, drain current (I_{DS}) can be described with the following equation:

$$I_{\text{DS}} = \mu(W/2L)C_i(V_G - V_T)^2$$

where C_i is the capacitance per unit area of the gate dielectric layer, V_G is the gate voltage, V_T is the threshold voltage, μ is the field-effect mobility, and W and L are the channel width and length dimensions, respectively. The mobility was calculated from the slope of the curve of $I_{\text{DS}}^{1/2}$ vs V_G (see Figure 7b). The threshold voltage of the device was determined from the linear fit of the square root of I_{DS} at the saturated regime vs V_G , and V_G was determined by extrapolating the measured data to $I_{\text{DS}} = 0$.

The film on the OTS-modified SiO_2/Si substrates shows small domains (see Figure 7b), which might have positive effect on the charge transportations as that observed in other polymers with high mobility. OFETs based on **PTZV-PT** afforded very high hole mobility up to $6.8 \times 10^{-3} \text{ cm}^2 \text{ V}^{-1} \text{ s}^{-1}$ with an on/off ratio of 2.5×10^4 and threshold voltage of -1 V. We fabricated 20 OFET devices, the mobility was in the range from 4.6×10^{-3} to $7.3 \times 10^{-3} \text{ cm}^2 \text{ V}^{-1} \text{ s}^{-1}$ with good reproducibility. Though the carrier mobility of **PTZV-PT** is not as good as those of the best devices such as regioregular poly(3-hexylthiophene) (0.01 – $0.1 \text{ cm}^2 \text{ V}^{-1} \text{ s}^{-1}$)^{7a} or some polymers with

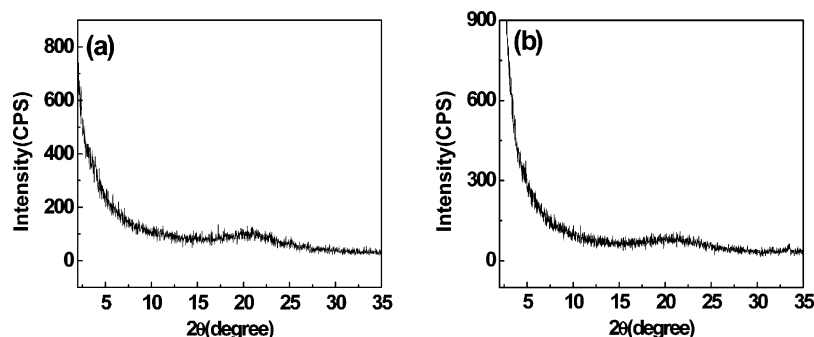


Figure 8. XRD patterns of spin-coated **PTZV-PT** thin films (50 nm thickness) on (a) SiO_2 surface and (b) OTS-modified SiO_2/Si substrates.

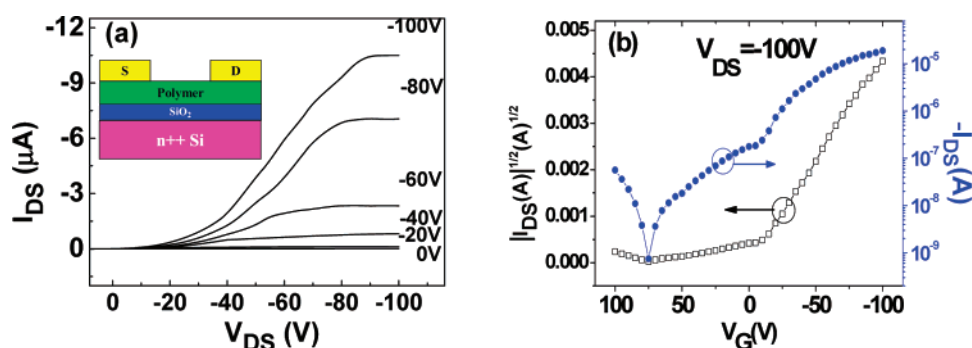


Figure 9. (a) Output and (b) transfer characteristics of **PTZV-PT** OFETs on OTS modified SiO_2 . I_{DS} was obtained at the drain voltage $V_{\text{DS}} = -100$ V for transfer characteristics. The drain-source channel length (L) and width (W) are $50\ \mu\text{m}$ and $3000\ \mu\text{m}$, respectively.

fused rings,^{7c,27} it is among the best performance of the OFETs based on the regiorandom polymers reported so far. In addition, further improvement of the mobility of **PTZV-PT** could be achieved by using more favorable device fabrication conditions (e.g., different solvents, surface treatment, thermal treatment, etc.). It has been reported that the conjugated polymers containing phenothiazine units possess more planar structure at excited-state than its ground state and are low-ionization potential polymer semiconductors.^{16,28} This may be the reason why higher hole mobility has been achieved for **PTZV-PT** even though the polymer films were in amorphous form. These results demonstrate that the conjugated polymers with phenothiazine-vinylene conjugated side chains are promising materials for high performance solution processable OFETs.

3. Conclusions

In summary, we have synthesized a new polythiophene derivative with conjugated phenothiazine-vinylene side chains, **PTZV-PT**, by the Stille coupling method. The polymer possesses good solubility in common organic solvents and high thermal stability. The UV-vis absorption spectra of the **PTZV-PT** film show a broad absorption band covering the wavelength range from 250 to 650 nm, which is composed of the absorption of the conjugated side chains (peaked at ca. 300 nm and at ca. 411 nm) and that of the conjugated main chains (peaked at around 535 nm). The PL spectra of **PTZV-PT** revealed that intramolecular exciton energy transfer occurred from the conjugated side chains to the main chains of the polymer. The hole mobility of the polymer measured by SCLC method reached $4.7 \times 10^{-3}\ \text{cm}^2\ \text{V}^{-1}\ \text{s}^{-1}$, which is a relatively higher value for conjugated polymers, indicating that the conjugated phenothiazine-vinylene side chains may promote the hole transportation of the polymer. OFETs based on **PTZV-PT** provide superior FET performance, affording a hole mobility of $6.8 \times 10^{-3}\ \text{cm}^2\ \text{V}^{-1}\ \text{s}^{-1}$ with an on/off ratio of 2.5×10^4 . These results suggest that the copolymers with phenothiazine-vinylene conjugated side chain represent a useful class of

solution processable semiconductors for fabrication of OFET circuits for printed electronics. The broad absorption and higher hole mobility indicate **PTZV-PT** could also be a promising polymer photovoltaic material.

4. Experimental Section

Materials. 3-Methyl thiophene was purchased from Aldrich Chemical Co, $\text{Pd}(\text{Ph}_3)_4$, $(\text{C}_4\text{H}_9)_3\text{SnCl}$, BuLi were obtained from Alfa Asia Chemical Co, and they were used as received. Tetrahydrofuran (THF) was dried over Na/benzophenone ketyl and freshly distilled prior to use. Toluene was dried over molecular sieves and freshly distilled prior to use. The other chemical reagents were common commercial level and used as received without further purification.

Synthesis of Monomers and Polymer. The synthetic routes of the monomers and polymer are shown in Scheme 2. The detailed synthetic procedures are as follows:

10-*n*-Octylphenothiazine (1). Phenothiazine (10 g, 50 mmol), sodium hydroxide (20.0 g, 500 mmol), and dimethyl sulfoxide (DMSO) (100 mL) were placed in a 250 mL two-necked flask, the mixture was stirred for half an hour, octyl bromide (7.7 mL, 55 mmol) was added dropwisely to the reaction mixture in 20 min, and then this mixture was stirred for 24 h at room temperature. The reaction mixture was poured into water, extracted with methylene chloride, and then dried with MgSO_4 . The resulting liquid was purified by column chromatography using petroleum ether as eluent. The product yield was 93% (13.2 g) as colorless liquid. MS: $m/z = 311\ (\text{M}^+)$. ^1H NMR (δ/ppm , CDCl_3): 7.11–7.09 (m, 4H), 6.89–6.80 (dd, 4H), 3.80–3.77 (t, 2H), 1.77 (d, 2H), 1.37–1.24 (m, 10H), 0.87 (t, 3H).

10-*n*-Octylphenothiazine-3-carbaldehyde (2). A 100 mL three-necked flask containing 10 mL (220 mmol) of anhydrous DMF was cooled in an ice bath. To this solution, 3 mL (32 mmol) of phosphorus oxychloride was added dropwisely for 30 min. Compound 1 (5.486 g, 17.64 mmol) in 30 mL of 1, 2-dichloroethane was added to the above solution and heated to ca. $90\ ^\circ\text{C}$ for 36 h. This solution was cooled to room temperature, poured into ice water, and neutralized to pH 6–7 by dropwise addition of saturated aqueous sodium hydroxide solution. The mixture was extracted with chloroform. The organic layer was dried with anhydrous MgSO_4 and then concentrated under reduced pressure. The crude product

was purified by column chromatography. The product was obtained (5 g, 84%) using petroleum ether and ethyl acetate (10:1) as the eluent by column chromatography under reduced pressure. FTIR (KBr, cm^{-1}): 2730 (s, $-\text{CHO}$). MS: $m/z = 339$ (M^+). ^1H NMR (δ/ppm , CDCl_3): 9.71 (s, 1H), 7.56 (d, 1H), 7.50 (s, 1H), 7.10–7.02 (m, 2H), 6.88 (t, 1H), 6.81 (t, 2H), 3.82 (t, 2H), 1.77 (q, 2H), 1.28 (m, 10H), 0.85 (m, 3H). Anal. Calcd for $\text{C}_{21}\text{H}_{25}\text{NSO}$: C, 74.33; H, 7.37; N, 4.13. Found: C, 74.21; H, 7.28; N, 4.11.

(2,5-Dibromothiophen-3-ylmethyl)phosphonic Acid Diethyl Ester (3). Compound **3** was synthesized with the route reported in ref 29, the crude product was purified by flash column chromatography eluting with petroleum ether/ethyl acetate (1:1). After purification, compound **3** was recovered as a pale yellow oil (22 g, 70% yield). MS: $m/z = 390$ (M^+). ^1H NMR (δ/ppm , CDCl_3): 7.00 (s, 1H), 4.08 (m, 4H), 3.10 (d, 2H), 1.29 (t, 6H).

2,5-Bis(tributylstannyl)thiophene (5). This compound was synthesized by a literature procedure.^{13a} GC-MS: $m/z = 664$. Yield: 72%. Purity (by GC-MS) $\geq 96\%$. ^1H NMR (δ/ppm , CDCl_3): 7.34 (s, 2H), 1.60 (m, 12H), 1.39 (m, 12H), 1.09 (m, 12H), 0.91 (t, 18H). Anal. Calcd for $\text{C}_{28}\text{H}_{56}\text{SSn}_2$: C, 50.78; H, 8.52. Found: C, 50.12; H, 8.75.

Synthesis of Polymer PTZV-PT. $\text{Pd}(\text{PPh}_3)_4$ (50 mg, 0.043 mmol), monomer **4** (0.594, 1.03 mmol), and monomer **5** (0.69 g, 1.03 mmol) were put into a three-necked flask. The mixture was flushed with argon for 10 min, and then 18 mL of toluene was added. At the protection of argon, the reactant was heated to reflux for 12 h. The mixture was cooled to room temperature and poured into 30 mL of methanol and then filtered into a Soxhlet thimble. Soxhlet extractions were performed with methanol, hexane, and CHCl_3 . The polymer was recovered from the CHCl_3 fraction by rotary evaporation. The solid was dried under vacuum overnight. The dark-purple polymer of **PTZV-PT** was obtained for 350 mg (yield: 68%). ^1H NMR (δ/ppm , CDCl_3): 7.36–7.08 (br, 7H), 6.82–6.52 (br, 5H), 3.74–3.71 (br, 2H), 1.74–1.72 (br, 2H), 1.22 (br, 10H), 0.97–0.82 (br, 3H). ^{13}C NMR (δ/ppm , CDCl_3): 144.7, 131.6, 127.3, 124, 122.3, 115.2, 114.9, 47.5, 31.9, 29.6, 26.7, 22.9, 14.1. Anal. Calcd For $(\text{C}_{30}\text{H}_{29}\text{S}_3\text{N})_n$: C, 72.14; H, 5.81; N, 2.81. Found: C, 72.04; H, 5.74; N, 2.76. M_w : 5.4×10^4 . PDI: 1.48.

Instruments and Measurements. ^1H NMR spectra were recorded using a Bruker AM-400 spectrometer, with tetramethylsilane (TMS) as the internal reference, chemical shifts were recorded in ppm. Elemental analysis was measured on a Flash EA 1112 elemental analyzer. Fourier transforms infrared (FT-IR) spectra were recorded on a BIO FTS-135 spectrometer by dispersing samples in KBr disks. Molecular weight and polydispersity of polymers were determined by gel permeation chromatography (GPC) analysis with polystyrene as standard (Waters 515 HPLC pump, a Waters 2414 differential refractometer, and three Waters Styragel columns (HT2, HT3, and HT4)) using THF as eluent at a flow rate of 1.0 mL/min at 35 °C. Thermogravimetric analysis (TGA) was conducted on a Shimadzu DTG-60 thermogravimetric analyzer with a heating rate of 10 K/min under a nitrogen atmosphere. Differential scanning calorimetric measurements (DSC) of the polymer was performed under nitrogen at a heating rate of 20 K/min with a Perkin-Elmer DSC-7 instrument. The UV-vis absorption spectra were recorded on a JASCO V-570 spectrophotometer. The photoluminescence (PL) spectra were obtained with a JASCO FP-6600 Fluorescence spectrophotometer. The structures of the polymer films were investigated by a SPI 3800N atomic force microscope (AFM) in

contacting mode with a 1 μm scanner. X-ray diffraction (XRD) measurements of the polymer thin film were carried out with a 2 kW Rigaku X-ray diffraction system. XRD patterns were obtained using Bragg-Brentano geometry ($\theta-2\theta$) with $\text{Cu K}\alpha$ radiation as an X-ray source in the reflection mode at 45 kV and 300 mA. The cyclic voltammogram was recorded with a Zahner IM6e electrochemical workstation (Germany) using polymer film on platinum disk as the working electrode, platinum wire as the counter electrode and Ag/Ag^+ (0.1 M) as the reference electrode in a nitrogen-saturated acetonitrile (CH_3CN) solution containing 0.1 mol/L tetrabutylammonium hexafluorophosphate (Bu_4NPF_6).

Fabrication of OFET Devices. Thin-film OFETs were fabricated with top-contact configuration. An n-doped Si wafer with a 450 nm thick thermally grown silicon dioxide layer (capacitance of 10 nF/cm²) was used as the substrate. The substrates were cleaned in water, alcohol, acetone, and rinsed in deionized water, and then modified by OTS. Thin polymer films were prepared by spin-coating of a 0.3 wt % solution of **PTZV-PT** in chloroform onto the OTS-modified SiO_2/Si substrates at a speed of 2500 rpm (revolutions per minute) for 40 s at room temperature. After the sample was dried at 80 °C and annealed at 155 °C under N_2 for half an hour, gold film (50 nm) was deposited on the organic layer to form the drain and source electrodes; for a typical device, the drain-source channel length (L) and width (W) are 50 μm and 3000 μm respectively. OFET measurements were performed at room temperature using a HP 4140B semiconductor parameter analyzer under ambient conditions.

Acknowledgment. This work was supported by NSFC (Nos. 20474069, 20421101, 50633050, 50673093 and 90206049) and the Ministry of Science and Technology of China (973 Project, No. 2002CB613404).

References and Notes

- (a) Kim, Y. K.; Cook, S.; Choulis, S. A.; Nelson, J.; Durrant, J. R.; Bradley, D. D. C. *Chem. Mater.* **2004**, *16*, 4812. (b) Liu, J. S.; Tanaka, T.; Sivula, K.; Alivisatos, A. P.; Fréchet, J. M. J. *J. Am. Chem. Soc.* **2004**, *126*, 6550. (c) Wienk, M. M.; Turbiez, M. G. R.; Struijk, M. P.; Fonrodona, M.; Janssen, R. A. J. *Appl. Phys. Lett.* **2006**, *88*, 153511.
- Thompson, B. C.; Kim, Y. G.; Reynolds, J. R. *Macromolecules* **2005**, *38*, 5359.
- Shi, C. J.; Yao, Y.; Yang, Y.; Pei, Q. B. *J. Am. Chem. Soc.* **2006**, *128*, 8980.
- Hou, Q.; Zhou, Q.; Zhang, Y.; Yang, W.; Yang, R.; Cao, Y. *Macromolecules* **2004**, *37*, 6299.
- Nicholson, P. G.; Ruiz, V.; Macpherson, J. V.; Unwin, P. R. *Chem. Commun.* **2005**, 1052.
- Lim, E.; Jung, B. J.; Shim, H.-K. *Macromolecules* **2003**, *36* (12), 4288.
- (a) Bao, Z.; Dodabalapur, A.; Lovinger, A. J. *Appl. Phys. Lett.* **1996**, *69*, 4108. (b) Bao, Z.; Lovinger, A. J. *Chem. Mater.* **1999**, *11*, 2607. (c) Young, K. M.; Lim, E.; Kang, I.-N.; Jung, B.-J.; Lee, J.; Koo, B. W.; Do, L.-M.; Shim, H.-K. *Macromolecules* **2006**, *39*, 4081. (d) Chang, J. F.; Sun, B. Q.; Breiby, D. W.; Nielsen, M. M.; Sölling, T. I.; Giles, M.; McCulloch, I.; Sirringhaus, H. N. *Chem. Mater.* **2004**, *16*, 4772.
- (a) Li, Y.; Wu, Y.; Ong, B. S. *Macromolecules* **2006**, *39*, 6521. (b) Ong, B. S.; Y. L. Wu.; Liu, P.; Gardner, S. J. *Am. Chem. Soc.* **2004**, *126*, 3378. (c) Zhu, Y.; Champion, R. D.; Jenekhe, S. A. *Macromolecules* **2006**, *39*, 8712. (d) Zhu, Y.; Babel, A.; Jenekhe, S. A. *Macromolecules* **2005**, *38*, 7983.
- (a) Crone, B.; Dodabalapur, A.; Gelperin, A.; Torsi, L.; Katz, H. E.; Lovinger, A. J.; Bao, Z. *Appl. Phys. Lett.* **2001**, *78*, 2229. (b) Bao, Z. *Adv. Mater.* **2000**, *12*, 227.
- Blanchet, G. B.; Loo, Y.; Rogers, J. A.; Gao, F.; Fincher, C. R. *Appl. Phys. Lett.* **2003**, *82*, 463.
- (a) Qiu, Y.; Hu, Y.; Dong, G.; Wang, L.; Xie, J.; Ma, Y. *Appl. Phys. Lett.* **2003**, *83*, 1644. (b) Pannemann, C.; Diekmann, T.; Hilleringmann, U. *J. Mater. Res.* **2004**, *19*, 1999.
- Wang, Y.; Zhou, E. J.; Liu, Y. Q.; Xi, H. X.; Ye, S. H.; Wu, W. P.; Guo, Y. L.; Di, C. A.; Sun, Y. M.; Yu, G.; Li, Y. F. *Chem. Mater.* **2007**, *19*, 3361–3363.
- (a) Hou, J. H.; Huo, L. J.; He, C.; Yang, C. H.; Li, Y. F. *Macromolecules* **2006**, *39*, 594. (b) Hou, J. H.; Yang, C. H.; Li, Y. F. *Synth. Met.* **2005**, *153*, 93. (c) Zhou, E. J.; He, C.; Tan, Z. A.; Hou, J. H.; Yang, C. H.; Li, Y. F. *J. Polym. Sci., Part A: Polym. Chem.* **2006**, *44*, 4916.

- (14) (a) Hou, J. H.; Yang, C. H.; He, C.; Li, Y. F. *Chem. Commun.* **2006**, 871. (b) Hou, J. H.; Tan, Z. A.; Yan, Y.; He, Y. J.; Yang, C. H.; Li, Y. F. *J. Am. Chem. Soc.* **2006**, *128*, 4911. (c) Hou, J. H.; Tan, Z. A.; He, Y. J.; Yang, C. H.; Li, Y. F. *Macromolecules* **2006**, *39*, 4657.
- (15) Zhou, E. J.; Tan, Z. A.; Huo, L. J.; He, Y. J.; Yang, C. H.; Li, Y. F. *J. Phys. Chem. B* **2006**, *110*, 26062.
- (16) Hwang, D.-H.; Kim, S.-K.; Park, M.-J.; Lee, J.-H.; Koo, B.-W.; Kang, I.-N.; Kim, S.-H.; Zyung, T. *Chem. Mater.* **2004**, *16*, 1298.
- (17) (a) Gomurashvili, Z.; Crivello, J. V. *Macromolecules* **2002**, *35*, 2962. (b) Simokaitiene, J.; Danilevicius, A.; Grigalevicius, S.; Grazulevicius, J. V.; Getautis, V.; Jankauskas, V. *Synth. Met.* **2006**, *156*, 926.
- (18) (a) Tamoto, N.; Adachi, C.; Nagai, K. *Chem. Mater.* **1997**, *9*, 1077. (b) Kulkarni, A. P.; Kong, X.; Jenekhe, S. A. *Macromolecules* **2006**, *39*, 8699. (c) Kong, X. X.; Kulkarni, A. P.; Jenekhe, S. A. *Macromolecules* **2003**, *36*, 8992. (d) Cho, N. S.; Park, J. H.; Lee, S. K.; Lee, J. H.; Shim, H. K.; Park, M. J.; Hwang, D. H.; Jung, B. J. *Macromolecules* **2006**, *39*, 177.
- (19) Sun, X.; Liu, Y.; Xu, X.; Yang, C.; Yu, G.; Chen, S.; Zhao, Z.; Qiu, W.; Li, Y.; Zhu, D. *J. Phys. Chem. B* **2005**, *109*, 10786.
- (20) (a) Lai, R. Y.; Kong, X.; Jenekhe, S. A.; Bard, A. J. *J. Am. Chem. Soc.* **2003**, *125*, 12631. (b) Lin, J.; Berkman, C. E.; Cashman, J. R. *Chem. Res. Toxicol.* **1996**, *9*, 1183.
- (21) Wadsworth, W. S.; Emmons, W. D. *J. Am. Chem. Soc.* **1961**, *83*, 1733.
- (22) Theander, M.; Inganäs, O. *J. Phys. Chem. B* **1999**, *103*, 7771.
- (23) Lee, Y. Z.; Chen, X.; Chen, S. A.; Wei, P. K.; Fann, W. S. *J. Am. Chem. Soc.* **2001**, *123*, 2296.
- (24) Li, Y. F.; Cao, Y.; Gao, J.; Wang, D. L.; Yu, G.; Heeger, A. J. *Synth. Met.* **1999**, *99*, 243.
- (25) Sun, Q. J.; Wang, H. Q.; Yang, C. H.; Li, Y. F. *J. Mater. Chem.* **2003**, *13*, 800.
- (26) (a) Malliaras, G. G.; Salem, J. R.; Brock, P. J.; Scott, C. *Phys. Rev. B* **1998**, *58*, 13411. (b) Martens, H. C. F.; Brom, H. B.; Blom, P. W. M. *Phys. Rev. B* **1999**, *60*, 8489. (c) Yang, C. H.; Hou, J. H.; Zhang, B.; Zhang, S. Q.; He, C.; Fang, H.; Ding, Y. Q.; Ye, J. P.; Li, Y. F. *Macromol. Chem. Phys.* **2005**, *206*, 1311. (d) Roman, L. S.; Inganäs, O. *Synth. Met.* **2002**, *125*, 419.
- (27) (a) McCulloch, I.; M. Heeney; C. Bailey; Genevicius, K.; Macdonald, I.; Shkunov, M.; Sparrowe, D.; Tierney, S.; Wagner, R.; Zhang, W.; Chabinyc, M. L.; Kline, R. J.; McGehee, M. D.; Toney, M. *Nat. Mater.* **2006**, *5*, 328. (b) Pan, H. L.; Li, Y.; Wu, Y. L.; Liu, P.; Ong, B. S.; Zhu, S. P.; Xu, G. *Chem. Mater.* **2006**, *18*, 3237.
- (28) Yang, L.; Feng, J. K.; Ren, A. M. *J. Org. Chem.* **2005**, *70*, 5987.
- (29) Andersson, M. R.; Mamm, W.; Olinga, T.; Svensson, M.; Theander, M.; Inganäs, O. *Synth. Met.* **1999**, *101*, 11.

MA071402V